NUCL SCI TECH (2020) 31:1
https://doi.org/10.1007/s41365-019-0712-1

Radiation shielding design of a compact single-room proton therapy based on synchrotron

Jin-Long Wang[1] · L. Alberto Cruz[2] · Qing-Biao Wu[3,4] · Qiong Wang[5] · Yao Wei[6] · Hong-Kai Wang[7]

Received: 29 August 2019 / Revised: 21 October 2019 / Accepted: 27 October 2019 / Published online: 19 December 2019

Abstract A synchrotron-based proton therapy (PT) facility that conforms with the requirement of future development trend in compact PT can be operated without an energy selection system. This article demonstrates a novel radiation shielding design for this purpose. Various FLUKA-based Monte Carlo simulations have been performed to validate its feasibility. In this design, two different shielding scenarios (3-m-thick concrete and 2-m-thick iron–concrete) are proved able to reduce the public annual dose to the limit of 0.1 mSv/year. The calculation result shows that the non-primary radiation from a PT system without an inner shielding wall complies with the IEC 60601-2-64 international standard, making a single room a reality. Moreover, the H/D value of this design decreases from 2.14 to 0.32 mSv/Gy when the distance ranges from 50 to 150 cm from the isocenter, which is consistent with the previous result from another study. By establishing a typical time schedule and procedures in a treatment day for a single room in the simulation, a non-urgent machine maintenance time of 10 min after treatment is recommended, and the residual radiation level in most areas can be reduced to 2.5 μSv/h. The annual dose for radiation therapists coming from the residual radiation is 1 mSv, which is 20% of the target design. In general, this shielding design ensures a low cost and compact facility compared with the cyclotron-based PT system.

Keywords Proton therapy · Radiation shielding · Monte Carlo · FLUKA

1 Introduction

Typically, an inner shielding wall between a patient and accelerator/beam transport system (BTS) is built using the traditional shielding design of a proton therapy (PT) facility [1]. Some new compact single-room solutions still have shielding walls between the patient and machine, for example, IBA Proteus ONE [2] and Varian ProBeam [3]. For a cyclotron, an energy selection system (ESS) for clinical applications is usually necessary. ESS generates high energy neutrons, thus requiring thick shielding walls around it. However, MEVION S250 has a compact design without inner shielding, and this system complies with the IEC 60601-2-64 standard [4].

Synchrotron can extract protons with different energies, as directly required by the treatment plan system, indicating that a synchrotron-based PT system can work without ESS. It enables the design of an even more compact proton

This work is partially supported by the China Postdoctoral Science Foundation (No. 2019M650611).

✉ Hong-Kai Wang
wanghongkai@chinansc.cn

[1] Guangzhou Concord Cancer Center, Guangzhou 510045, China

[2] University of Florida, Gainesville, FL 32611, USA

[3] Institute of High Energy Physics, Chinese Academy of Science (CAS), Beijing 100049, China

[4] Spallation Neutron Source Science Center, Dongguan 523803, China

[5] National Supercomputing Center, Wuxi 210008, China

[6] Union Hospital, Tongji Medical College, Huazhong University of Science and Technology, Wuhan 430022, China

[7] Nuclear and Radiation Safety Center, Ministry of Ecology and Environment, Beijing 102400, China

facility without an inner shielding wall [5] to be possible. The Radiance 330 synchrotron, which is produced by ProTom, can be installed within an interior accelerator vault space of 54 m^2 and requires up to 40% less radiation shielding than many other systems currently in the market. The compact synchrotron designs by Hitachi PROBEAT and Mitsubishi in Japan show a trend toward more compact and simple designs [3].

According to the reports of International Commission on Radiological Protection [6] and National Council on Radiation Protection and Measurement [7], the occupational and annual public dose limits are 20 and 1 mSv, respectively. The same values are also provided in Chinese Standard GB18871-2002 [8]. The standard (GBZ/T 201-2007) requires that the dose rate at 30 cm outside the shielding wall should be less than 2.5 μSv/h [9]. For a conservative design, the shielding design used in the present study is listed in Table 1. The occupational exposure is 5 mSv (one-fourth of the standard), and exposure to the public is 0.1 mSv (one-tenth of the standard). The dose limit rate at 30 cm outside the treatment room is 1.5 μSv/h. Note that the dose here is the ambient dose equivalent expressed in sievert unit.

Section 201.10.2.101.4.3 of the IEC 60601-2-64 standard prescribes the dose limit for a patient in the treatment area [10]. The maximum absorbed dose in the range of 15–50 cm laterally away to the beam axis is not allowed to exceed 0.5% of the dose amount delivered at the isocenter. In the patient plane with a lateral distance in the range of 50–200 cm, the maximum absorbed dose from all radiation types must be below 0.1% of the dose delivered at the isocenter. Note that the dose here represents the absorbed dose expressed in gray unit.

To evaluate the dose level and effects of a compact synchrotron-based single-room PT system on the environment and patient, it is necessary to profoundly understand the radiation sources during the shielding design process. These radiation sources represent the locations where the proton beam interacts with matters, i.e., the bending dipoles, injection/extraction units, nozzle, and treatment volume.

The aims of the present study are to calculate the dose or dose rate distribution of an entire facility and to verify whether the design can provide a radiation shield within the threshold value. The effects of non-primary radiation on the patient and the residual radiation on the occupational staff are calculated and evaluated.

Table 1 Dose limit

Dose limit type	Standard	Objective
Occupational dose limit	20 mSv/year	5 mSv/year
Public dose limit	1 mSv/year	0.1 mSv/year
Dose rate limit	2.5 μSv/h	1.5 μSv/h

2 Materials and methods

FLUKA, as a general Monte Carlo (MC) toolkit, is adopted to calculate the dose distribution, and it has been verified by many other experiments [11–13]. SimpleGEO and Flair, which are advanced interfaces for FLUKA, are designed to create complex MC model and to analyze data [14, 15]. The typical time consumption for a primary particle number of 10^6 is 1–2 h on a standalone computer with a single core (Intel Core (TM) i7-8550U CPU @ 1.8 GHz and 16 GB memory). The multi-thread parallel computing at the National Supercomputing Center in Wuxi is therefore required to reduce the statistical error to less than 10%. With 1000 cores (SW26010) used in the calculation, the time consumption can be reduced to less than 10 h if the primary number is set to 10^{10} [16].

To obtain an accurate dose distribution and to verify whether the shielding design satisfies the requirement of the target limit listed in Table 1, a simplified geometry model with an accelerator, beam transport line, and nozzle is constructed and simulated in FLUKA. The layout is shown in Fig. 1. The target is a water sphere with a radius of 20 cm at the isocenter. The beam path of the scanning nozzle is a helium chamber. The BTS contains three bending magnets. The extraction and injection system consist of several septa. The synchrotron has four bending dipoles. The scanning nozzle is composed of two dipoles. The beam path chamber and two ion chambers are filled with argon gas.

Table 2 lists the beam losses of the major sources shown in Fig. 1. The quadrupole magnets, steering magnets, acceleration cavity, and beam profile monitors are not considered because the beam loss at these positions is very significantly lower than that of the dipole magnet. The beam loss in the vacuum tubes is normalized to the nearby dipoles. The energy of the injection proton is 3.5 MeV. The source from the injection can be ignored in all dose calculations as it contributes little to the total dose. The transmission contribution represents a conservative estimation compared with that in some other similar studies [17, 18], and it can be defined as a relative value with respect to the current at a certain point. For the extraction and synchrotron cases, the conservative transmission values (70% and 50%, respectively) are provided because a lot of protons are lost during the commissioning.

To simulate the proton-transport process, synchrotron and BTS dipole magnets are set with a magnet field. The four synchrotron dipole magnets (D1–D4) equally share

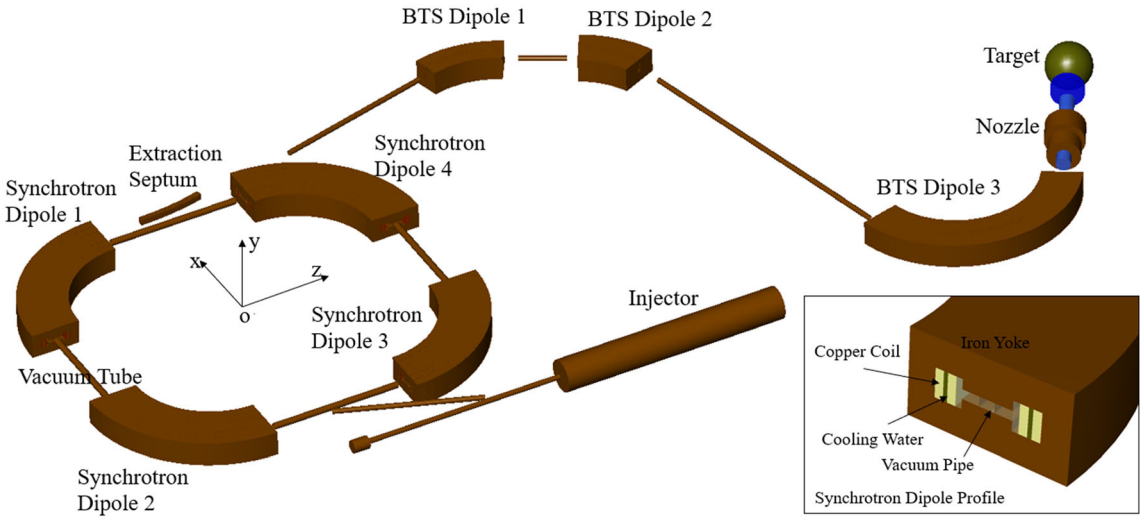

Fig. 1 (Color online) MC geometry model of the synchrotron-based PT system

Table 2 Beam loss table

Source	Material	Transmission (%)	Energy (MeV)	Input current (nA)	Loss current (nA)
Target	Water	0	130–230	2.00	2.00
Nozzle	Helium	95	130–230	2.11	0.11
BTS	Iron	90	130–230	2.34	0.23
Extraction	Iron	70	130–230	3.34	1.00
Synchrotron	Iron/copper	50	130–230	6.68	3.34

50% of the beam losses, and the three BTS dipole magnets (D1–D3) share only 10% of the beam losses. Four gantry angles (G0: 0°, G1: 90°, G2: 180°, and G3: 270°) share 100% of the losses in the target. Table 3 lists the beam loss weight of the different sources for every injected proton. We can summarize that the synchrotron and extraction beam losses have a relatively high weight. These sources will be considered in a detailed model, and the evaluation of their influence on the patients, occupational staff, and environment is presented in the following sections.

For the annual dose calculation, an average current of 1 nA and the weight of the proton energy are considered. The energy weight used in the calculations is listed in Table 4 [19].

The annual workload for a single treatment room is calculated by using Eq. (1). The conditions under which the calculation is performed are listed in Table 5. Thus, the estimation of the maximum annual workload is 500 nA h.

$$\text{Workload} = \text{Patients} \times \text{Fields} \times \frac{\text{Time per field}}{60\ \text{min/h}} \times \text{Current} \times \text{Working days} \quad (1)$$

Table 4 Energy weight

Energy (MeV)	Weight
230	0.176
210	0.140
180	0.123
160	0.313
130	0.248

Table 3 Beam loss weight

Synchrotron				Extraction	BTS			Nozzle	Target			
D1	D2	D3	D4		D1	D2	D3		G0	G1	G2	G3
0.125	0.125	0.125	0.125	0.15	0.0117	0.0117	0.0117	0.0158	0.0748	0.0748	0.0748	0.0748

Table 5 Annual workload

Parameters	Value
Patients per day	30
Working day per year	250
Fields per patient	2
Time per field (min)	2.00
Average beam current (nA)	1.00
Daily workload (nA h)	2.00
Annual workload (nA h)	500.00

For the dose rate distribution calculation, a maximum current of 2 nA at the target and high energy case are considered. For a patient in the treatment area, the deepest modulated spread-out Bragg peak (SOBP: 25–33 cm) obtained from several individual Bragg peaks at staggered depths is used to calculate the absorbed dose [19].

3 Results of general shielding

3.1 Annual dose limit

Concrete ($\rho = 2.3$ g/cm^3) and iron ($\rho = 7.87$ g/cm^3) are well-known basic materials for PT facility shielding [20, 21]. For a standard design, only concrete is used, and the shielding layout is shown in Fig. 2.

The dose equivalent distribution is shown in Fig. 3. The three lines with different colors represent different thresholds for our objective [(0.1 mSv/year: pink), requirement in the US standard (1 mSv/year: purple), and the occupational limit (5 mSv/year: blue)]. We can conclude that the thickness of the concrete wall should not be less than 2 m to reduce the dose below 0.1 mSv/year except in the region close to the isocenter, which requires a thicker wall (3 m) to shield the prompt radiation. The left panel in Fig. 3 shows that the value at the maze door is slightly above the threshold prescribed in the standard, indicating that the public should stay away from the maze exit during treatment. The 1.5-m-thick wall is able to reduce the dose to the US standard; that will save a lot space if such system can be installed. For the occupational staff, this shielding design is also sufficient.

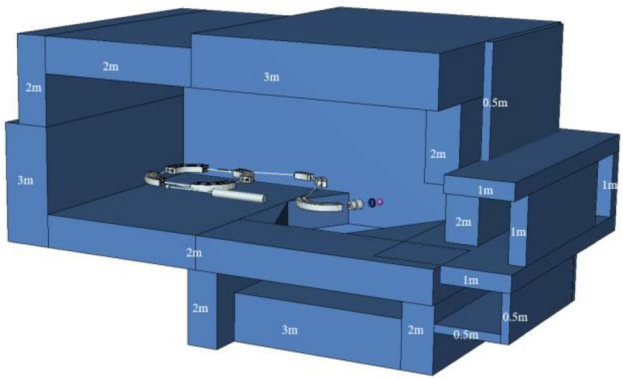

Fig. 2 (Color online) Layout of the concrete shielding design

The design that combines mixed concrete and iron can be an excellent solution to the problem caused by space limits. The geometry implemented in the simulation is shown in Fig. 4. Iron with a maximum thickness of 1 m is used to shield high energy neutrons, while hydrogenous materials are to shield low energy neutrons. The dose equivalent map based on this design is shown in Fig. 5. It is worth noting that it is different from Fig. 3 because iron plates with different thicknesses (in black) are placed at different positions in the treatment room. In this case, the high density of the iron plates allows the maximum thickness of the wall to be reduced to 2 m. The three color lines that represent the different thresholds can also be well constrained in the shielding wall, which proves that the combined design provides a similar shielding ability to the design shown in Fig. 3.

3.2 Dose rate limit

For a conservative design, a maximum current of 2 nA at the target and an 8-cm-deep SOBP created by the method mentioned in Ref [22] are applied to calculate the dose rate distribution. Figure 6 shows that the pink envelope line, indicating the objective limit value of 1.5 μSv/h is within the shielding limit in both cases. The shielding complies with the requirement of the GBZ/T 201-2007 standard.

4 Results of the Inner Shielding Wall

4.1 Modulated SOBP

To measure the absorbed dose required by the IEC standard, a deepest 8-cm SOBP is generated by the weight adaption method by using Eq. (2) [20]. The black curve in Fig. 7 shows the simulated dose distribution according to the range weight, which is marked with the blue curve. Here, the lateral field size is 5 × 5 cm^2, and the absorbed dose at the SOBP flat top is 2 Gy.

$$W(R) = \begin{cases} \rho D_0 \dfrac{P \sin(\pi/P)\alpha^{1/P}}{\pi (d_{\max} - R)^{1/P}} \left(\dfrac{1}{a + bR}\right)^k, & d_{\min} \le R < d_{\max} \\ 0, & R < d_{\min},\ R \ge d_{\max} \end{cases} \quad (2)$$

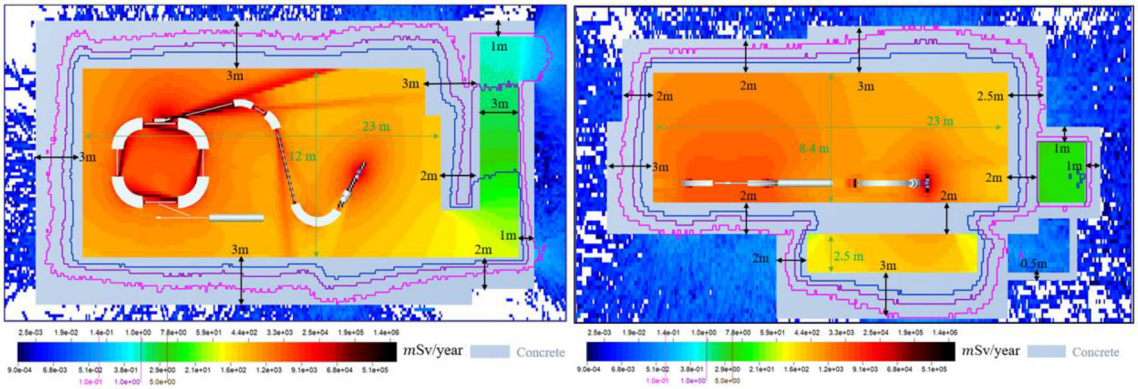

Fig. 3 (Color online) Annual dose equivalent distribution of the concrete shielding. Left: horizontal *XZ* plane at $Y = 0$ cm. Right: vertical *YZ* plane at $X = -60$ cm. The pallet shows the dose distribution from 9×10^{-4} to 1.4×10^{6} mSv/year

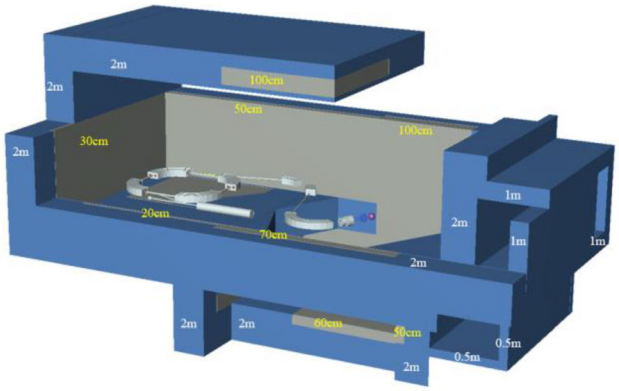

Fig. 4 (Color online) Design that combines (blue) mixed concrete and (gray) iron

The fitted parameter values are $\alpha = 420.4812$, $P = 1.73825$, $a = 4.49$, $b = -0.08945$, and $k = 2.2$.

4.2 Non-primary radiation and inner shielding wall

The proton loss during the beam transport process generates secondary particles such as neutrons and gammas. They are not intended to treat a patient and may cause risk in the clinic. Thus, a proper mitigation method must be considered to deal with the non-primary radiation.

The non-primary radiation outside the projection of the radiation field is measured at six locations, namely A1, A2, B1, B2, C1, and C2. The different locations of these measurements are shown in Fig. 8. A1 and A2 are mirror of each other located at a lateral distance of 15 cm outside the radiation field. The other two pairs (B1, B2 and C1, C2) have a similar layout but at farther lateral distances, which are 50 and 200 cm, respectively.

A1 and A2 are inside the target water sphere. To obtain the contribution weight of the non-primary radiation, each source in Table 2 is separately simulated, which is a distinct process. The values of the non-primary radiation at A1 and A2 are listed in Table 6, which indicate that the target and nozzle contribute more than 99% of the absorbed dose, whereas the contributions from the other sources are three orders of magnitude lower. The total non-primary radiation dose is 5.37×10^{-3} Gy, accounting for 0.27% of the field dose of 2 Gy. This ratio is significantly lower than that of the IEC standard requirement (0.5%).

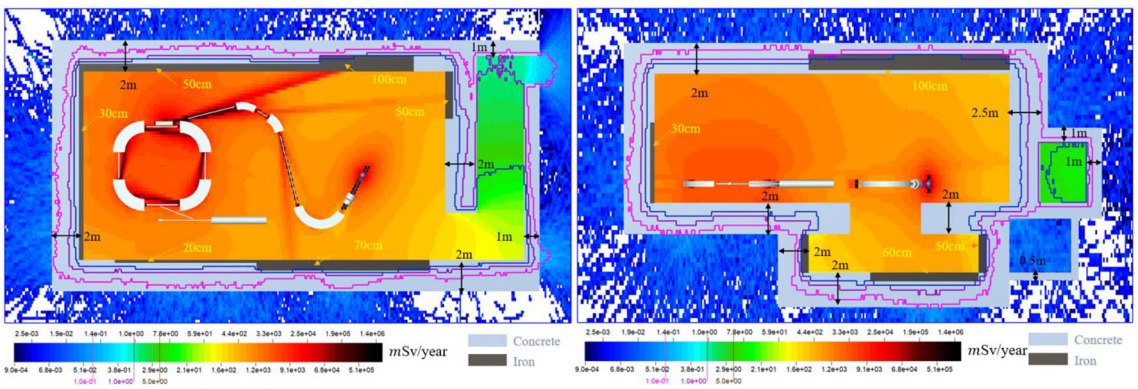

Fig. 5 (Color online) Annual dose equivalent distribution of (gray) mixed concrete and (black) iron shielding. Left: horizontal *XZ* plane at $Y = 0$ cm. Right: vertical *YZ* plane at $X = -60$ cm. The pallet shows the dose distribution from 9×10^{-4} to 1.4×10^{6} mSv/year

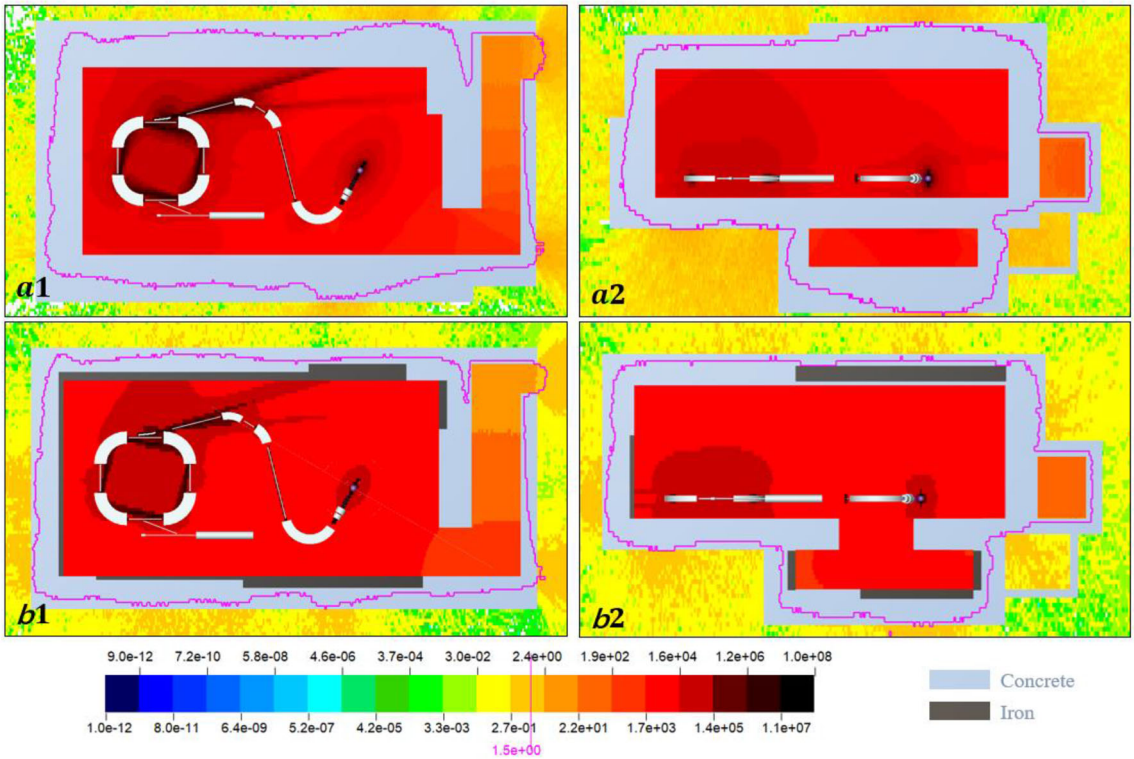

Fig. 6 (Color online) Upper row: a1 and a2 represent the dose rate distribution of the concrete shielding in horizontal and vertical views, respectively. Bottom row: Dose rate distribution of mixed concrete and iron shielding. b1 represents the horizontal view, and b2 represents the vertical view

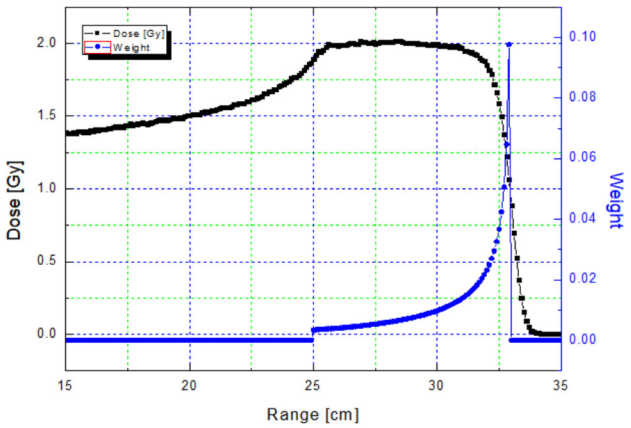

Fig. 7 (Color online) An 8-cm-deep SOBP generated by the weight adaption method

The non-primary radiation data at distances of 50 and 200 cm outside the radiation field are listed in Table 7. For B1 and B2, the target and nozzle contribute approximately 99% of the non-primary radiation. According to the result at closer distances to the machine, the contribution of the extraction and synchrotron points at C1 significantly increases in which total non-primary radiation doses are 0.07% and 0.003%, respectively. This ratio is also smaller than the IEC standard requirement, which is 0.1%.

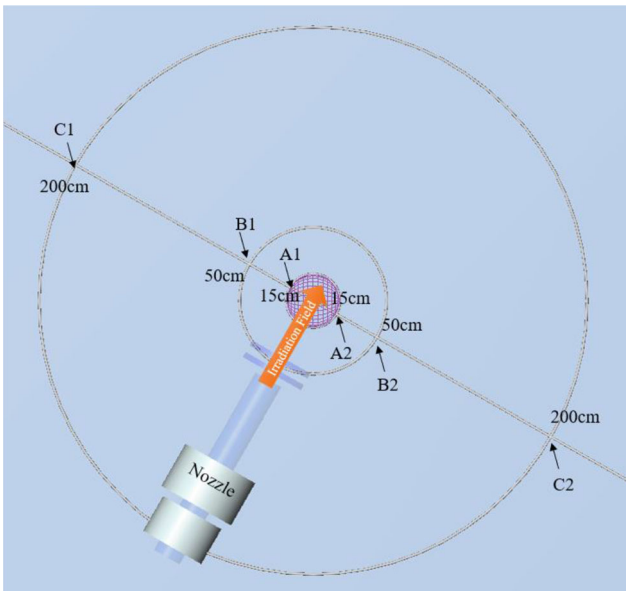

Fig. 8 (Color online) Locations of the measurement points of the non-primary radiation outside the radiation field

According to the calculation results, a conclusion can be drawn that the synchrotron-based compact proton facility can feasibly work without an inner shielding wall. To verify this conclusion, we investigate three other

Table 6 Non-primary radiation at 15 cm outside the radiation field

Region	15 cm			
Source	A1		A2	
	Absorbed dose (Gy)	Weight (%)	Absorbed dose (Gy)	Weight (%)
Target and nozzle	5.35×10^{-3}	99.60	5.54×10^{-3}	99.63
BTS	7.98×10^{-6}	0.15	1.04×10^{-5}	0.19
Extraction	7.62×10^{-6}	0.14	5.15×10^{-6}	0.09
Synchrotron	5.85×10^{-6}	0.11	4.99×10^{-6}	0.09
Sum of all sources	5.37×10^{-3}	100.00	5.56×10^{-3}	100.00
Ratio to the field dose	0.27%		0.28%	

Table 7 Non-primary radiation at 50 and 200 cm outside the radiation field

Region	50 cm				200 cm			
Source	B1		B2		C1		C2	
	Absorbed dose (Gy)	Weight (%)	Absorbed dose (Gy)	Weight (%)	Absorbed dose (Gy)	Weight (%)	Absorbed dose (Gy)	Weight (%)
Target and nozzle	1.48×10^{-3}	98.98	1.26×10^{-3}	99.17	4.12×10^{-5}	68.33	4.40×10^{-5}	81.57
BTS	5.80×10^{-7}	0.04	7.58×10^{-7}	0.06	5.66×10^{-7}	0.94	4.51×10^{-7}	0.84
Extraction	8.88×10^{-6}	0.60	4.50×10^{-6}	0.35	1.24×10^{-5}	20.63	4.53×10^{-6}	8.40
Synchrotron	5.75×10^{-6}	0.39	5.28×10^{-6}	0.42	6.08×10^{-6}	10.10	4.96×10^{-6}	9.20
Sum of all sources	1.49×10^{-3}	100.0	1.27×10^{-3}	100.0	6.03×10^{-5}	100.0	5.40×10^{-5}	100.0
Ratio to field dose	0.07459%		0.06349%		0.00301%		0.00270%	

configurations with different inner shielding walls: 10-cm concrete, 2-cm iron and 5-cm concrete, and 2-cm iron and 5-cm concrete local shielding walls. Figure 9 shows that the inner wall can shield radiation that comes from the synchrotron and extraction processes. To be specific, the 2-cm iron and 5-cm concrete shielding wall can shield the radiation from the extraction process in a more efficient manner.

However, the inner shielding wall obviously does not change the dose distribution around the target, as listed in Table 8. The reason is that the target and nozzle contribute most of the non-primary radiation at locations A1, B1, and C1. Although a patient does not benefit from the inner wall, which means it is unnecessary to build such a wall for a synchrotron-based compact proton facility, a local shielding wall is still recommended because this little addition can reduce the radiation from the extraction process.

4.3 H/D value

H/D value is defined as the dose equivalent per therapeutic dose, which is calculated by using Eq. (3). It is an important quantitative index to evaluate the non-primary radiation level around the patient.

$$\frac{H}{D}\left(\frac{\text{mSv}}{\text{Gy}}\right) = \frac{\text{FLUKA Scoring dose equivalent (mSv)}}{\text{Field dose 2 Gy}} \tag{3}$$

The H/D distribution of the configuration without an inner wall is shown in Fig. 10. The H/D value decreases from 2.14 to 0.32 mSv/Gy when the distance from the isocenter ranges from 50 to 150 cm. From the comparison with the literature, the different settings and results of the H/D value are listed in Table 9, which shows that the H/D value relatively matches the result by Polf et al.

5 Results of residual radiation

In this section, we present the evaluation of the residual radiation and its influence on the radiation therapist (RT). The typical time schedule and procedures in a treatment day in a single room are listed in Table 10. Each patient treatment consists of three steps, namely 2 min of field

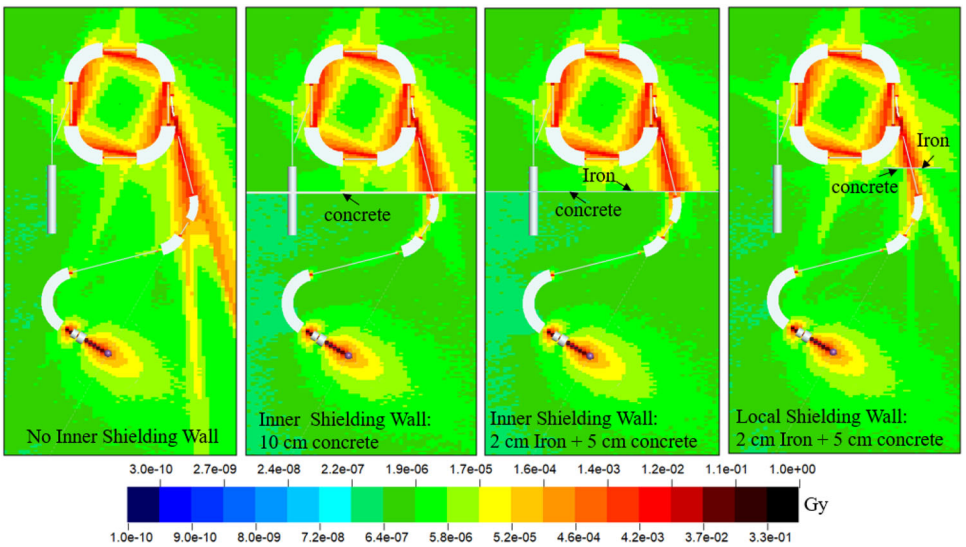

Fig. 9 (Color online) Dose distribution of four different inner shielding wall configurations

Table 8 Non-primary radiation of the different configurations

Configuration	A1 (Gy)	B1 (Gy)	C1 (Gy)
No inner wall	5.37×10^{-3}	1.49×10^{-3}	6.03×10^{-5}
10-cm concrete	5.00×10^{-3}	1.34×10^{-3}	5.41×10^{-5}
2-cm iron and 5-cm concrete	4.80×10^{-3}	1.22×10^{-3}	5.77×10^{-5}
Local shielding	5.78×10^{-3}	6.03×10^{-4}	5.29×10^{-5}

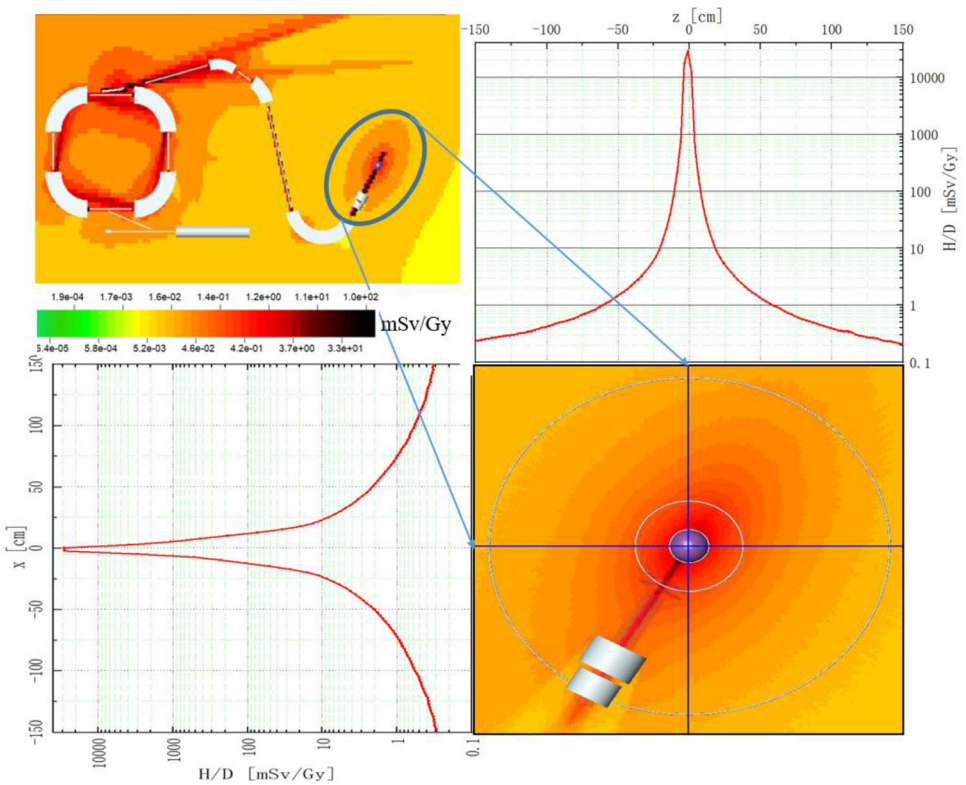

Fig. 10 (Color online) H/D value distribution

Table 9 H/D values from different studies

	Present study	Rebecca et al. [23]	Polf et al. [24]	Chen et al. [25]
H/D value	2.14–0.32 mSv/Gy	2.27–3.95 mSv/Gy	2.3–0.51 mSv/Gy	4.59–0.30 mSv/Gy
Position	50–150 cm from isocenter	50 cm from isocenter	50–150 cm from isocenter	50–150 cm from isocenter
Data	FLUKA simulated	Measured	MCNPX simulated	MCNPX simulated
Beam	8-cm SOBP	Passive scattering clinical beam	Passive scattering 8.5-cm SOBP	Passive scattering 10-cm SOBP
Accelerator	Synchrotron	Synchrocyclotron (Mevion)	–	Synchrocyclotron (Mevion)

irradiation, 2 min of beam-off repositioning, and another 2 min of field irradiation. The average current is 1 nA, and each field dose is 2 Gy. The RT has to get into the treatment room to reposition and discharge every patient. During these 4 min, the therapist must approach the patient and is thus exposed to the residual radiation coming from the patient and the device.

Figure 11 shows that when the treatment of the 30th patient is finished, the residual radiation is counted from 10 s to 8 h. Figure 11 shows that the target, extraction, and synchrotron ring are the most intense residual radiation sources. For several minutes at the start, the dose rate level around these sources is 1–100 μSv/h but rapidly decays afterward. After cooling down to approximately 10 min, the machine sources show a higher level than the target because the half-life of the target-produced radionuclides is shorter than the machine-produced radionuclides [19]. The radiation level in most areas in the single room is reduced to 2.5 μSv/h after 10 min of cooling, which is a relatively safe level for non-urgent machine maintenance activities. Urgent maintenance is allowed immediately after treatment. However, the results demonstrate that the operators should stay more than 50 cm away from the extraction components few minutes from the start or use tools to handle the hot components in the machine.

The Z profile of the residual dose rate around the target is shown in Fig. 12. Here, the Z profile is defined as the dose rate as a function of the Z axis centered at the isocenter. The left panel represents the profile between 10 s and 2 min of cooling. The dose rate at the isocenter immediately after the treatment can reach up to approximately 700 μSv/h. At the distance of 25 cm from the isocenter, the value decays to ∼ 30 μSv/h and reaches approximately 1 μSv/h at 200 cm. The middle panel shows the same profile at cooling times from 2 min to 1 h. Even though the isocenter dose rate decays from ∼ 100 to ∼ 10 μSv/h, this value still indicates a high level for the patient companions; hence, they should stay at least 1 m from the patient. The right panel shows the Z profile from 1 to 8 h of cooling. The patient dose rate falls down to 10 μSv/h or even lower, indicating that the companions can safely approach the patient.

The RT is exposed to residual radiation when repositioning and unloading the patients, and the patient companions are exposed to residual radiation from the patient. To calculate the integrated dose, the dose rate at each cooling time is measured ∼ 25 cm away from the isocenter, as shown in Fig. 13. The result indicated by the orange area, which represents the integrated dose for the RT from 0 to 120 s, is 1.30 μSv. The integrated dose

Table 10 Typical treatment day in a single room

Time	Action	Beam on/off	Role	Duration (min)
6:00	Morning QA	On	Medical physicist	60
7:00	Bringing first patient to treatment room	Off	Radiation therapist	1
7:01	Patient loading and positioning	Off	RT	11
7:12	First field treatment	On	RT	2
7:14	Patient repositioning	Off	RT	2
7:16	Second field treatment	On	RT	2
7:18	Patient unloading	Off	RT	2
7:20	Second patient treatment		RT	20
7:40	Third to thirtieth patient treatment		RT	560
22:00	End of treatment day			

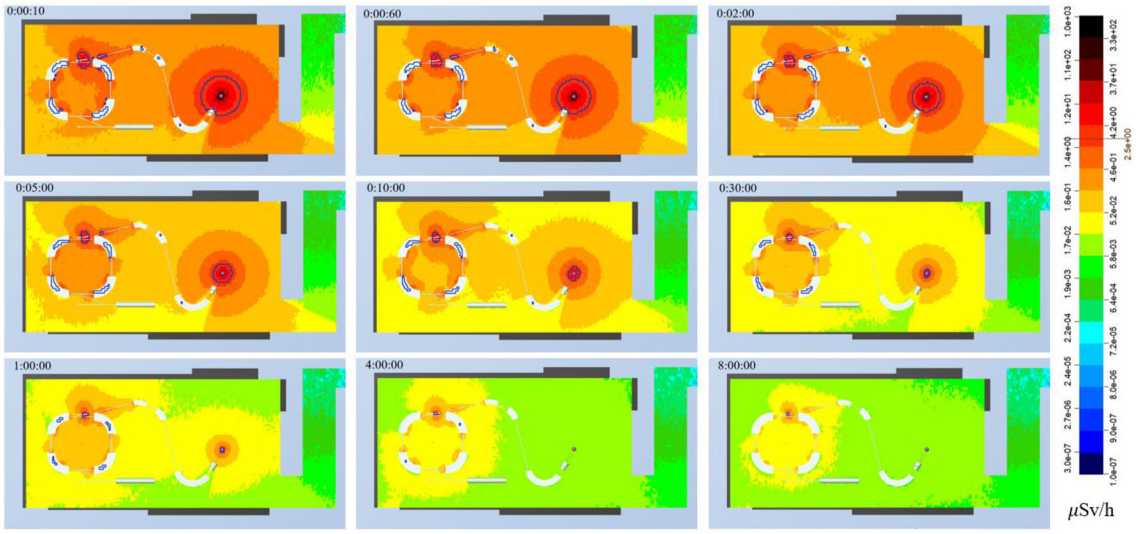

Fig. 11 (Color online) Residual radiation distribution

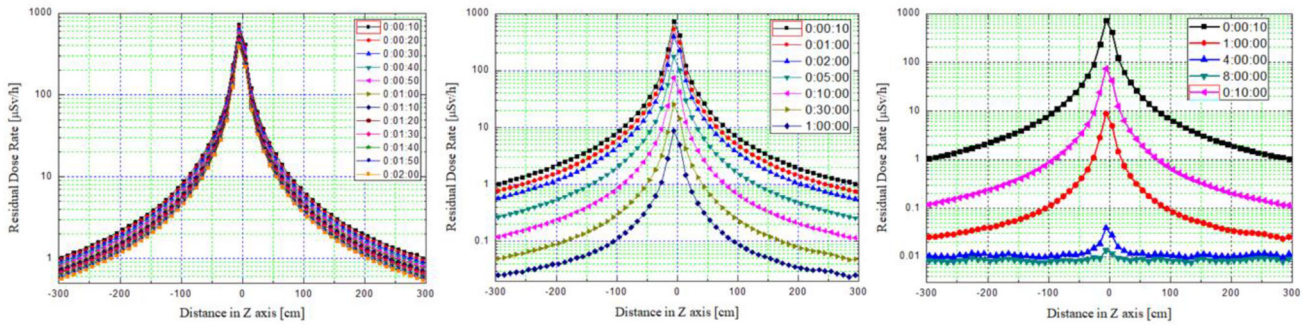

Fig. 12 (Color online) Residual dose rate profile of the target under different cooling time intervals

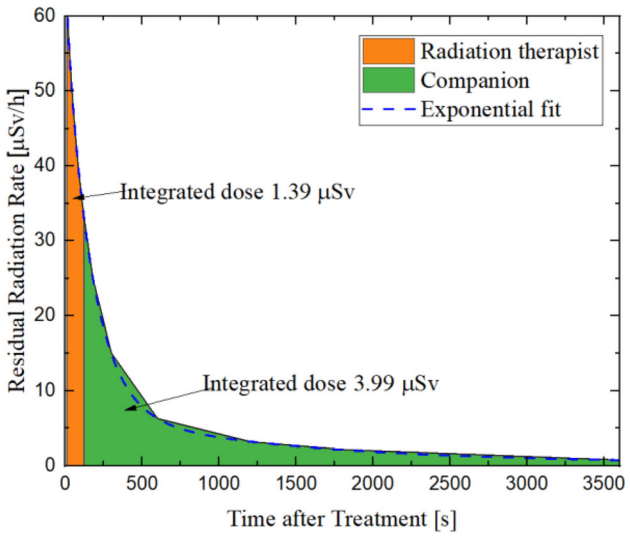

Fig. 13 (Color online) Integrated residual dose for the RTs and patient companions. The integrated dose is fitted using an exponential function

indicated by the green area is 3.99 μSv for the patient companions from 2 min to 1 h.

Typically, two RTs are present in a single room per day. Every RT handles 15 patients per day. Thus, the annual dose that the RTs received from residual radiation can be calculated using Eq. (4), which is 1.04 mSv. This value is one-fifth of the designed target value (5 mSv) and is significantly lower than the standard limit value of 20 mSv.

$$\text{RT annual residual dose} = 1.39\ \mu\text{Sv} \times \text{fields} \times \text{patients} \times \text{working days} \tag{4}$$

If the patient treatment is divided into 30 fractions, the total dose of the patient companion can be calculated using Eq. (5), which is 0.1197 mSv. If the patient has several companions, the dose can be equally distributed to a relatively lower level per person.

$$\text{Companion total residual dose} = 3.99\ \mu\text{Sv} \times \text{fractions} \tag{5}$$

6 Conclusion

In this study, detailed calculations have been performed to validate the feasibility of a new compact PT facility. The results prove that a PT system with a compact synchrotron-based single room satisfies the requirements of radiation protection standards with its compact shielding. Specifically, two different shielding designs (a 3-m concrete or 2-m iron–concrete shielding wall) can attenuate the annual target dose limit value of 0.1 mSv/year, and a 1.5-m concrete or 1-m iron–concrete shielding wall can attenuate the annual dose to the standard limit value of 1 mSv. This design reveals the advantages of reduced footprint and cost compared with the cyclotron-based PT system.

Without ESS, the non-primary radiation from the machine is maintained at a low level and satisfies the IEC 60601-2-64 international standard, which means that a synchrotron-based proton facility can be operated without an inner shielding wall, making a compact single room a reality. However, a local shielding wall is still recommended because the radiation distribution can be optimized with little additional effort.

The calculated H/D value decreases from 2.14 to 0.32 mSv/Gy when the distance from the isocenter is from 50 to 150 cm. This low-level H/D distribution is consistent with the previous results in the literature.

A 10-min non-urgent machine maintenance time for everyday treatment is recommended so that the residual radiation level in most areas in the single room can be reduced to $\sim$ 2.5 μSv/h. Urgent maintenance is allowed immediately after treatment. However, the workers should stay at least 50 cm away from the extraction components a few minutes from the start or use tools to handle the hot components in the machine.

The received annual dose for RTs from residual radiation is 1.04 mSv, which is approximately one-fifth of the design target of 5 mSv and much lower than the standard limit value of 20 mSv. The results also show that the received annual dose for the patient companion from residual radiation is 0.1197 mSv. If the patient has several companions, this dose is shared, resulting in a lower level.

Acknowledgements The authors would like to thank Dr. Andrii Rusanov for the user routine application of the FLUKA simulations and rich knowledge of particle physics. The authors would also like to thank Sheng Peng, Zhengzheng Liu, and Zhihong Zheng for their knowledge on PT and accelerator physics. Qiming Lu, Desheng Zhang, Jiarong Su, and Huosheng Ruan shared their vast experience in the 3D model and building construction that greatly helps our work. We also sincerely thank Micheal Lu for the many discussions about imaging device in PT. Finally, we would like to thank the National Supercomputing Center for providing the cluster resources, especially Wei Zhang, Yongbin Zhang, and Yong Yang for their effort in the coding tests and other support.

References

1. PTCOG Report1. Sub-Committee Task Group on Shielding Design and Radiation Safety of Charged Particle Therapy Facilities, (2010). https://www.ptcog.ch/archive/Software_and_Docs/Shielding_radiation_protection.pdf. Accessed 18 Oct 2019
2. F. Stichelbaut, M. Closset, Y. Jongen, Secondary neutron doses in a compact proton therapy system. Radiat. Prot. Dosim. **161**, 1–4 (2014). https://doi.org/10.1093/rpd/ncu028
3. M. Schillo, Global industrial development of accelerators for charged particle therapy, in *Proceedings of the 5th International Particle Accelerator Conference, Dresden, Germany*, 15–20, June, 2014, https://doi.org/10.18429/jacow-ipac2014-weib01
4. U. Linz (ed.), *Ion Beam Therapy. Biological and Medical Physics, Biomedical Engineering* (Springer, Berlin, 2012). https://doi.org/10.1007/978-3-642-21414-1
5. M.T. Gillin, N. Sahoo, M. Bues et al., Commissioning of the discrete spot scanning proton beam delivery system at the University of Texas M.D. Anderson Cancer Center, Proton Therapy Center, Houston. Med. Phys. **37**, 154–163 (2010). https://doi.org/10.1118/1.3259742
6. A.D. Wrixon, New ICRP recommendations. J. Radiol. Prot. **28**, 161–168 (2008). https://doi.org/10.1088/0952-4746/28/2/R02
7. NCRP Report No. 144, Radiation Protection for Particle Accelerator Facilities, vol. 113, (2005), p. 456. https://doi.org/10.1093/rpd/nch479
8. National Standard, GB18871-2002, Basic standards for protection against ionizing radiation and for the safety of radiation sources
9. National Standard, GBZ/T 201-2007, Radiation shielding requirements in room of radiotherapy installations
10. International Standard, IEC 60601-2-64. Medical electrical equipment: Particular requirements for the basic safety and essential performance of light ion beam medical electrical equipment
11. A. Ferrari, P. Sala, A. Fasso et al., Fluka: a multi-particle transport code. Technical Report (2005). https://doi.org/10.2172/877507
12. T.T. Böhlen, F. Cerutti, M.P.W. Chin et al., The fluka code: developments and challenges for high energy and medical applications. Nucl. Data Sheets **120**, 211–214 (2014). https://doi.org/10.1016/j.nds.2014.07.049
13. E.V. Bellinzona, M. Ciocca, A. Embriaco et al., A model for the accurate computation of the lateral scattering of protons in water. Phys. Med. Biol. **61**, 102–117 (2016). https://doi.org/10.1088/0031-9155/61/4/N102
14. C. Theis, K.H. Buchegger, M. Brugger et al., Interactive three dimensional visualization and creation of geometries for Monte Carlo calculations. Nucl. Instrum. Methods A. **562**, 827–829 (2006). https://doi.org/10.1016/j.nima.2006.02.125
15. V. Vlachoudis. FLAIR: A Powerful But User Friendly Graphical Interface For FLUKA, in Proceedings of International Conference on Mathematics, Computational Methods and Reactor Physics, Saratoga Springs, New York, (2009)

16. P.G. Chin, J.P. Giddy, D.G. Lewis et al., An embarassingly parallel framework for running EGSnrc/BEAMnrc/DOSXYZnrc, FLUKA, MCNP/MCNPX, GEANT4 and PENELOPE on grid and cluster computers, in Proceedings of 15th International Conference on the Use of Computers and Radiotherapy, Toronto, (2007)
17. S. Agosteo, G. Arduini, G. Bodei et al., Shielding calculation for a 250 MeV hospital-based proton accelerator. Nucl. Instrum. Methods A. **374**, 254–268 (1996). https://doi.org/10.1016/0168-9002(96)00017-4
18. J. Xu, X. Xia, G. Wang, J. Lv, Radiation calculations for advanced proton therapy facility, in Proceedings of the 4th International Particle Accelerator Conference. Shanghai, 12–17 May 2013. https://doi.org/10.1128/jvi.06227-11
19. Q. Wu, Q. Wang, T. Liang, Study on patient-induced radioactivity during proton treatment in hengjian proton medical facility. Appl. Radiat. Isotopes **115**, 235–250 (2016). https://doi.org/10.1016/j.apradiso.2016.06.029
20. S. Agosteo, M. Magistris, A. Merehetti et al., Shielding data for 100–250 MeV proton accelerators: double differential neutron distributions and attenuation in concrete. Nucl. Instrum. Methods B **265**, 581–598 (2007). https://doi.org/10.1016/j.nimb.2007.09.046
21. S. Agosteo, M. Magistris, A. Merehetti et al., Shielding data for 100–250 MeV proton accelerators: attenuation of secondary radiation in thick iron and concrete/iron shields. Nucl. Instrum. Methods B **266**, 3406–3416 (2008). https://doi.org/10.1016/j.nimb.2008.05.002
22. J. Wang, C. Alberto, Z. Liu et al., Weight adaption-based spread-out Bragg peak method. Chin. J. Med. Phys. **36**, 50–54 (2019). https://doi.org/10.3969/j.issn.1005-202X.2019.01.010
23. M. Rebecca, Measured neutron spectra and dose equivalents from a Mevion single-room, passively scattered proton system used for craniospinal irradiation. Int. J. Radiat. Oncol. **95**, 249–257 (2016). https://doi.org/10.1016/j.ijrobp.2015.12.356
24. J.C. Polf, W.D. Newhauser, Calculations of neutron dose equivalent exposures from range-modulated proton therapy beams. Phys. Med. Biol. **50**, 3859–3873 (2005). https://doi.org/10.1088/0031-9155/50/16/014
25. K. Chen, C. Bloch, H. Hill et al., Evaluation of neutron dose equivalent from the mevion S250 proton accelerator: measurements and calculations. Phys. Med. Biol. **58**, 8709–8723 (2013). https://doi.org/10.1088/0031-9155/58/24/8709